RJC

RASĀYAN *J. Chem.*
Vol. 18 | No. 3 |1385-1393| July-September | 2025
ISSN: 0974-1496 | e-ISSN: 0976-0083 | CODEN: RJCABP
http://www.rasayanjournal.com
http://www.rasayanjournal.co.in

FABRICATION OF Al-5052/Al_2O_3/MoS_2 HYBRID COMPOSITES FOR BETTER MECHANICAL AND ELECTROCHEMICAL PROPERTIES

K. V. Anil Kumara[1,2,✉], R. D. Prutviraj[2] and M. T. Swamy[2,3]
[1]Department of Chemistry, Sai Vidya Institute of Technology,
Bangalore-560064, Karnataka, India
[2]Department of Chemistry and Research in Chemistry, Raja Rajeswari College of Engineering
(affiliated to Visveswaraya Technological University, Belagavi-590018),
Bangalore- 560074, Karnataka, India
[3]Department of Chemistry, Sambhram Institute of Technology,
Bangalore-560097, Karnataka, India
✉Corresponding author: anilkumara.kv@saividya.ac.in

ABSTRACT

Aluminium alloys are utilized in sectors such as aerospace and automotive due to their combined tremendous power and light mass. Moreover, when Aluminum alloys encounter various conditions, such as temperature fluctuations, corrosion can significantly limit their lifespan. This article investigates the use of Alumina (Al_2O_3) and ash from palm kernel shells as particles of reinforcement in the Al 5052 matrix alloy, focusing on the corrosion behavior of hybrid composites at different mixing ratios. The stir casting technique is used to create the composites. The tensile strength and hardness of the resulting composites were evaluated. Both gravimetric and electrochemical techniques were utilized to investigate the rusting behavior of the composites in solutions containing NaCl. The results from the gravimetric analysis indicated that the composite film had defects and that corrosion products were developing on the exteriors of the specimens. The reinforcements of the Al 5052 matrix acted as active locations where rusting can start. The samples' electrochemical corrosion behavior was analysed and depicted by the Bode and Nyquist graphs, which linked for primary surface responses to charge transfer processes. The results of our research work show that the usage of composites in locations less susceptible to corrosion attack will be made possible by the improved protection in application regions.

Keywords: Gravimetric, Alumina, Tensile Strength, Al 5052 Matrix, Nyquist and Bode.
RASĀYAN *J. Chem.*, Vol. 18, No. 3, 2025

INTRODUCTION

Numerous scientific research discoveries have contributed to the ongoing advancement of innovative engineering materials utilized in the automotive, building construction, aviation, and marine industries.[1,2] Matrix classification is used to classify composite materials, which constitute a significant portion of sophisticated engineering materials.[3] One class of composite materials that is comparable to advanced engineering materials is the matrix of metal composites (MMC). As base matrices, several metal matrices, including Ti, Mg, and Al, have all been utilized. On the other hand, most research has been done on an aluminium matrix composite (AMCs) due to its mechanical properties.[4] AMCs, or Aluminum matrix composites, were versatile resources used in mechanical engineering applications. AMCs have been the subject of a lot of recent efforts precisely of their low thickness, strong particular strength, and favourable ratio of mass to strength, good quality, and comparatively strong resistance to wear, Excellent physical, thermal and mechanical qualities have been linked to the implementation of AMCs in automobiles and aircraft industries[5]. In order to create the reinforcements, two different methods are used: either synthetic reinforcements (Al_2O_3, Al_2O_3 & B_4C, and TiC) or pairings of two artificial reinforcements or reinforcements made from utilizing agro-residue (RHA, BPA, CCA, SBA, and rice husk ash).[6] The mechanical and physical tribological characteristics of hybrid reinforced HCs have been extensively, and ascribed to

http://doi.org/10.31788/RJC.2025.1829327

multiple physical, chemical, or electrochemical correspondences involving the matrix and reinforcements, as well as the corrosive environment under simulation.[7] Results of our Al-5052/Al_2O_3/MoS_2 hybrid composites are in lined with the 9th SDG. i.e. Industry, innovation and infrastructure, protection technologies are crucial for achieving the overall SDGs. Prepared hybrid composites are useful for infrastructure development and the economic growth of the country. The corrosion behaviour of different AMCs made with Al_2O_3 and ash from palm kernel shells (MoS_2). The impact of MoS_2 and Al_2O_3 particles on the corrosion susceptibility of Al 5052/Al_2O_3/MoS_2 composites is not well understood. Thus, in this work, the vulnerability of corrosion to artificially manufactured AMCs in a Solution of sodium chloride at 3.5 weight percent was examined. Potentio dynamic polarization was investigated, and the composites' weight decrease in both solutions was calculated. The current article focuses on the enhancement of mechanical and electrochemical Al-5052/Al_2O_3/MoS_2 Hybrid composites.

Significance and Implications of the Research

Hybrid composites are significant for corrosion control due to their capacity to combine the strength and corrosion resistance of various materials. They can be customized for particular applications, offering advantages like weight reduction and improved mechanical properties, while effectively preventing corrosion in critical structural components.

EXPERIMENTAL

Production of Materials and Composites

The Al 5052 alloy is composed of various metals in different weight percentages. The intricate composition and properties of the composite are shown in the Table-1a and 1b.

Table-1a: Composition of Al 5052

Name	Composition in percentage by weight
Aluminium	97.25
Magnesium	2.2 - 2.5
Chromium	0.15 - 0.25
Copper	0.1
Iron	0.4
Manganese	0.1
Silicon	0.25
Zinc	0.1

Table-1b: Properties of Al 5052

Density	2.68 g/cm^3
Elastic Modulus	70.3 Gpa
Melting Point	607 °C
Specific Heat Capacity	880 J/Kg-K
Tensile Strength: Ultimate (UTS)	195 - 290 Mpa
Vickers Hardness	92 HV
Thermal Conductivity	138 W/Mk

For the production of Composites, the double stir casting method (liquid metallurgy) was employed. Using the charge calculation method, the MoS_2 and Al_2O_3 particulates needed for each composition in the matrix alloy were assessed. By preheating at 250 °C, inherent moisture was removed, and the reinforcement's wettability within the matrix was improved. In a gas-fired crucible, the matrix ignites were melted after being charged. At a temperature higher than the matrix alloy's liquid temperature (750 °C), this was done to ensure that the matrix alloy melted completely. After charging the heated reinforcement particles into a semi-solid molten matrix alloy, the slurry was manually agitated for a duration of five to ten minutes. After that, the slurry was heated to 800°C and given another mechanical stir at 400 rpm for a few minutes. The slurry was finally poured into a sand mould that had been prepared and left to solidify. After solidification, the composite product was then obtained.[8]

Preparation of Specimen

A sample of Ø30 × 3 mm was cut from each composition. Every sample was ground between 240 and 1000 grits of Al_2O_3 paper, cleaned with acetone, rinsed with water, and allowed to dry. A vernier gauge was used to determine the sample's thickness, and a digital electronic balance was used to measure the sample's weight. The samples' microstructures were investigated with a scanning electron microscope, TESCAN model for Vega 3. Emery paper was accustomed to polishing the composite specimens' surfaces. A Brinell hardness tester was then used to determine the specimens' Brinell hardness. ASTM E384 standards were used to test the three composite samples. A 50 kN capacity computer-controlled universal tensile machine (UTM) called INSTRON-3369 was utilized to measure the specimen's tensile strength. At room temperature, the composite specimens were treated at a crosshead speed of 0.5 mm/min. Tensile tests were carried out on the composite specimens in compliance with ASTM E8 specifications.[9]

Mechanical and Physical Characteristics

The physical characteristics of the composites, namely their density and porosity, were ascertained.[10] Nonetheless, the ASTM E10-18 standard was used to calculate the composites' Brinell hardness value. [11] to ensure data reliability, the average hardness value of each sample's four indentations was used. By the ASTM E8 standard, a 5 mm diameter sample and a 30 mm gauge length were used for the tensile test.[12] A strain rate of 0.5mm/min was employed utilizing a universal testing machine (UTM) (Instron 3369, model number). To ensure the accuracy of the data, the curation process is used. The average values of hardness and Tensile test were plotted in Fig.-1. These obtained values are in agreement with the other studies, like Reddy *et al.,* and Jainesh *et al.*

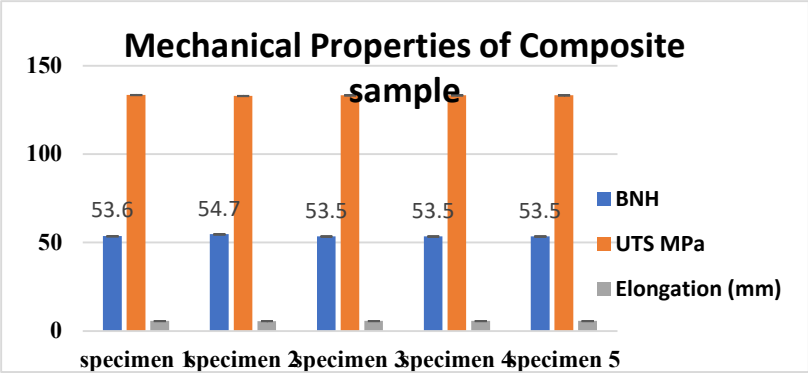

Fig.-1: Hardness and Tensile Test Result

Isiaka Oluwole OLADELE and Avwerosuoghene Moses OKORO found that adding treated PKSA to Aluminium alloy results in robust composites suitable for automobile applications. The study found that treated PKSA strengthened the Al matrix phase more effectively than untreated PKSA due to increased adhesion between the two materials. Similarly, the tensile strength and hardness of the composites showed a significant increase in this investigation.

Corrosion Test

Gravimetric Measurement and the Immersion Test

To determine the Al composites' hybrid corrosion rate, weight loss was determined with 0.1 mg accuracy using a digital scale. A solution of 3.5 weight percent NaCl was employed to create the corrosive environment. Each sample was weighed before being individually dipped in the two solutions. The specimens were removed from the solutions. Cleaned as well as dried before reweighing. This process was conducted at room temperature for fifteen days. Weight loss rates and corrosion rates expressed in millimetres per year (mm/year) were computed. The deteriorated surfaces are inspected using photographs. To prevent evaporation, a cover made of glass was put over the container containing the specimens in the corrosion test at extreme temperatures. The weight loss measured was computed utilizing ASTM G31-12a-based Equation (1), and the rate of corrosion was assessed using eqn.-2.

$$\text{Weight loss, } W = W^B - W^A \quad \text{Weight loss} \qquad (1)$$

$$\text{CPR} = \frac{K \times W}{D \times A \times T} \qquad \text{Corrosion rate} \qquad (2)$$

In this case, A stands for area (cm^2), W for weight loss (mg), D for material density (g/cm^3), T for exposure time (h), K for a constant (8.766 × 104), and CPR for corrosion rate (mm/year).

Electrochemical Corrosion Test

The produced composite was put through accelerated electrochemical tests. The potentio dynamic measurements were conducted at 25 °C utilizing a NaCl solution at 3.5 weight percent. The specimens were cleaned and polished to a 1 cm^2 surface area before being placed in the measuring vessel. Silver/Silver chloride (Ag/AgCl) acts as the electrode for reference, the Composite sample is the counter-electrode, and the working electrode is platinum. The equipment was set for about 30 minutes in order in order to attain the potential for corrosion (Ecorr) necessary for the test. The curves of anodic polarization were noted by applying an automated potential shift at a 10-3V rate. As stated in ASTM G102-89, at a scan rate, the polarization measurements were carried out of 0.0016 v/s between -1.5 and +1.5 V. The measurements were taken 24 and 72 hours after the different specimens were immersed in a 3.5 percent by weight NaCl solution. The log current versus potential Tafel plots is employed to determine the corrosion current and corrosion potential (Ecorr) & (Icorr) for each sample. The potentiodynamic apparatus was used to obtain the measurement using electrochemical impedance spectrometry (EIS), which was then used to acquire the Bode and Nyquist graphs.

RESULTS AND DISCUSSION

The Composite Product's Microstructure

The unreinforced matrix metal's microstructure is shown in Fig.-1a. The microstructure shows no signs of intermetallic grain. Figure-1b –1e shows the microstructures of a few more exemplary samples. Figures-1b and 1d, respectively, show the monolithic strengthened tiny structures samples of Al_2O_3 and MoS_2. However, Figures-1c,1e display the tiny structures of the representative samples of hybrid reinforced composites. The homogeneous allocation of reinforcement particles inside the matrix was evident. The composites that were created showed no signs of fracture development or increased pores because of the chosen handling methods and parameters utilized in the composite synthesis. There is a sign of favourable wetting conditions from the reinforcing particles to the matrix.[13] The micrographs displaying the evenly dispersed reinforcement particles validate the effectiveness of the twofold stir casting procedure in releasing tension at the surface that exists from the matrix alloy and the particles of reinforcement in the composite. Consequently, during the double stir casting procedures, trapped bubbles of air in the slurry are allowed to escape.

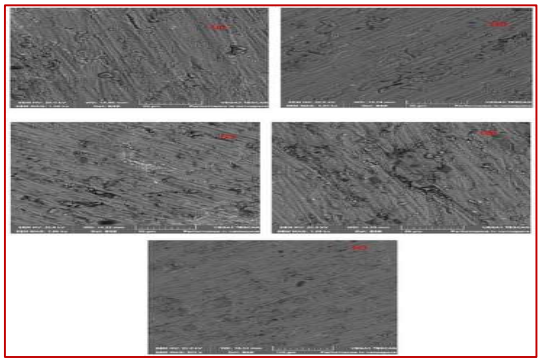

Fig.-1a-1e: Micrographs of Samples A0, A1, A5, A6, and A9 Taken with a Microscope that Uses Scanning Electrons

Physical and Mechanical Properties

The unreinforced alloy has a theoretical density of 2.7 g/cm^3 and a percentage porosity of 2.063%. Sample A1 had the maximum density (2.71 g/cm^3), while sample A5 had the least density (2.56 g/cm^3). Sample A6 came in second with 2.66 g/cm^3. The quantity of M_OS_2 elements within the matrix was the cause of the low density shown in samples A5 and A6. MoS_2 has a lower density than the matrix alloy and Al_2O_3. As a result, its presence lowers the composite's total density. However, due to the density of Al_2O_3 being higher than

the matrix, sample A1's density was greater than sample A0's. The density of sample A9 is greater due to the higher concentration of Al_2O_3 particles (8%) compared to MoS_2 particles (2%) in the sample. It is well known that the majority of biomass reinforcement particles have lower densities, which inevitably affects the composite's total density. The porosity percentage for each sample is smaller than 2.4%, indicating that the composites that are formed are within the acceptable range for cast hybrid composites (HCs).[14] Although the monolithic reinforced sample A6's minuscule 2 percent MoS_2 content generated a hardness value larger than sample A0 but less than sample A1, MoS_2 particles comprise hard phases of silica and other strengtheners. Much higher hardness values were obtained when Al_2O_3 and MoS_2 reinforcing particles were combined. A9, the sample with the highest hardness rating, contained 8% Al_2O_3 and 2% MoS_2. Certain intermetallic can be added to the composites to increase their hardness. A high dislocation density or a rise in the volume of precipitated phases indicates an increase in hardness. Therefore, when the surface area of the additional reinforcing particles grows, so does the matrix grain size. The samples generated were found to have an elongation percentage ranging from 5.0% to 7.6%. Sample A0, the unreinforced alloy, had the best percentage of elongation. Sample A9 exhibits the lowest percentage of elongation (5.0%), which may be ascribed to its capacity to sustain plastic strain due to the hard components found in the MoS_2 and Al_2O_3 particles. As a result, it was observed that the matrix's ductile phase and the composite's percentage elongation had decreased.[15]

Gravimetric Analysis:

Corrosion Behaviour in 3.5 Weight Percent NaCl Environment

The variations in weight and rates of corrosion of the specimens in a solution of 3.5% salt are shown against the sample exposure period in Fig.-2 and 3. Both weight gains and decreases are shown by the result fluctuations. Adhesive corrosion products may be the cause of the weight gain. Developing on the sample surfaces. As a result, the thermal expansion coefficient (CTE), Orowan strengthening methods, may momentarily decrease. On the other hand, the weight loss might result from the flaws in the films disintegrating over a few days and progressively removing reinforcements.

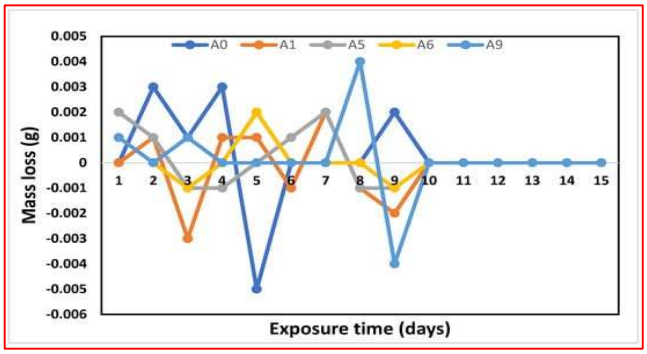

Fig.-2: Changes in Specimen Mass as a Function of Exposure in a Solution of 3.5 Weight Percent NaCl

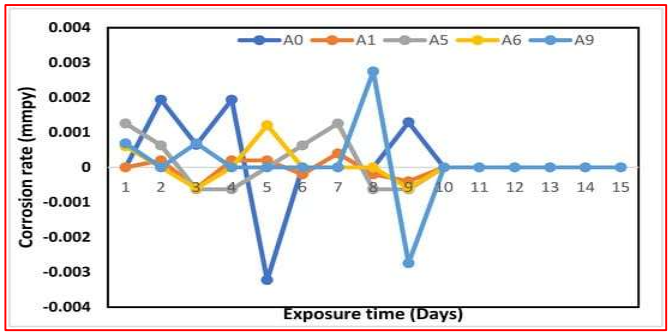

Fig.-3: Specimen Corrosion Rate as a Function of Exposure Duration in a 3.5 Weight Percent NaCl Solution

The NaCl solution at 3.5 mass percent has a mass loss of 0.04 grams. The composites may be appropriate for use in salty or marine settings with additional protection since they are nearly steady and have little

resistance to general corrosion in 3.5 weight percent NaCl. Comparable outcomes were found in this work and the research of Bodunrin and Alaneme[11,12,13], in which a reinforced-alumina Al 5052 matrix was submerged in 3.5 weight percent NaCl. Because the degree of the rate of corrosion was below 0.1 mmpy. The reinforcement addition had a somewhat different impact on the corrosion behaviour than the unreinforced matrix. The materials could be appropriate for usage in marine conditions based on the mass increase observed when the samples were measured gravimetrically. Because of the silica in MoS_2, the Al_2O_3 and Al interfacial interaction prevents the development of the Al_4C_3 phase, increasing the vulnerability of the matrix to corrosion.[14,15] This is because Aluminum is not melted in silica crucibles. Al_2O_3 and Al do not react; however, it is conceivable for intermetallic phases to develop that act as corrosion-initiation sites. Furthermore, the Al-Al_2O_3 composite is predicated on the reaction's absence.

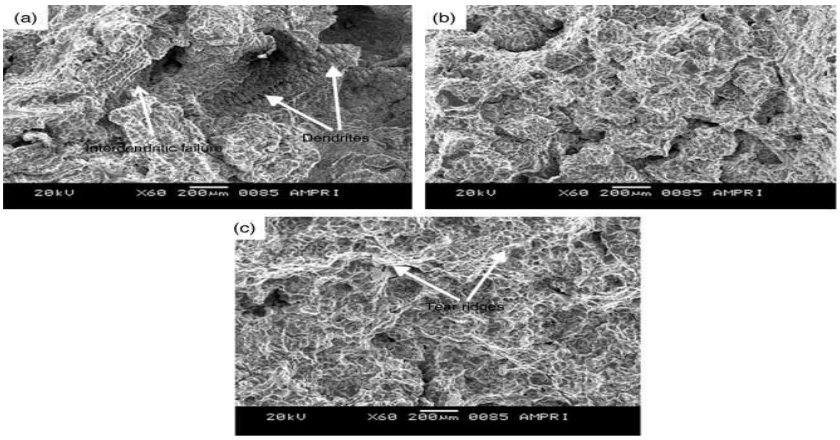

Fig.-4: (a) A9 and (b) A1 Samples that Were Corroded Following Being Submerged in a Solution of NaCl for Fifteen Days. Sample That was Not Corroded

Figure-4a, 4b displays the samples' surface after 15 days of exposure to a NaCl solution in comparison to the sample that was not submerged in the solution (Fig.-4c). All of the specimens exhibit comparable corrosion behaviors, including surges in both directions, both favourable and unfavourable, that evoke memories of observations made during possible measurements. Although the level of pH may be responsible for these results, the composites showed very little pitting corrosion in the 3.5 weight percent solution of NaCl (pH = 7.4). Cl ions start the pitting corrosion process in four (4) steps. Localized acidity results from the hydrolysis in the corrosion product, which is always coupled with the oxidation of metals in the corroding pits system. This confined acidity is maintained by the significant division of the anodic and cathodic half-reactions. Due to inadequate oxygen penetration, the electrolyte progressively becomes more acidic. Because of the acidity, anion electrons move toward the pit that is formed. The pits upon the metal's surface are often filled with the byproducts of the corrosion process. While anodic procedures start with the metal surface in contact with the electrolyte, the surface that surrounds the cathode has undergone passivation. Consequently, the reinforcing inclusions, which are particles from the second phase, appear on the metal surface. The precipitation-forming particles near grain boundaries potentially act as local anodes, leading to the creation of early pits and localized galvanic corrosion. It is possible for localized strains that appear as surface dislocations to develop into anodes and initiate pits. For instance, the metal's surface acts as a cathode and the anode-forming pits when exposed to a NaCl solution that contains a lot of oxygen. Eventually, the extra favorable charge produced by the cations of metal is attracted to the chloride anions in the electrolyte.

Electrochemical Measurement among the Specimens

Corrosion Behaviour in a 3.5 Weight Percent Solution of NaCl Using PDP

Figure-5a and Fig.-5b display Potentiodynamic polarization curves for the composite materials after they were exposed in a 3.5 weight percent solution of NaCl for 24 and 72 hours, respectively. Compared to reinforced specimens, which have an Ecorr of -A1, A5, A6, and A9 have respective voltages of 0.761 V, -0.885 V, -0.863 V, and -0.899 V. The obtained Ecorr of -0.22 V is nobler. The samples' reactions in NaCl

demonstrated how vulnerable they were to corrosion attacks. This supports the observations made during the gravimetric experiment. The Ecorr measured in 3.5% NaCl was -220.62 mV. Additionally, the reinforced specimens' corrosion potential and current, as displayed in Figure 5a, were comparatively low, with Icorr ranging from 5.45 to 40.87 µA/cm2 and Ecorr from -220.62 to -899.48 mV. Chloride attack at the aluminum–reinforcement interface might serve as the root cause of this phenomenon.

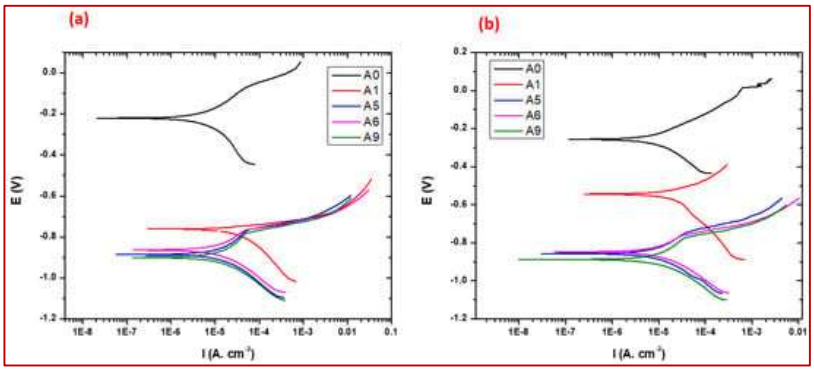

Fig.-5a-5b: The Composites' Polarization Curves at 24 and 72 Hours in a 3.5% Mass NaCl Solution

Table-3: Icorr and Ecorr Values for Samples

Sample Number	Composition
A1	Al 5052
A5	Al 5052/Al_2O_3 2%wt/ MoS_2 8%wt
A6	Al 5052/Al_2O_3 4%wt/ MoS_2 2%wt
A9	Al 5052/Al_2O_3 8%wt / MoS_2 2%wt

Table-3 shows Icorr and Ecorr A0, A1, A5, A6, and A9 sample values. The lowest was found in Sample A. Icorr value (5.45 µA/cm2) after 24 hours of immersion in a solution of NaCl, while Sample A5 had the least Icorr value (6.809 µA/cm2) after 72 hours. A low rate of corrosion in a NaCl solution is indicated by a low Icorr value. When submerged in a solution of NaCl, the unreinforced alloy's Icorr values increased from 24 hours (5.45 µA/cm2) to 72 hours (7.373 µA/cm2). This suggests that the unreinforced alloy's corrosion rate rose with exposure time, as was to be expected in a solution of NaCl. Several samples submerged in NaCl solution showed an increase in Icorr values,72 hours after exposure. As was previously mentioned, the exposure regime-dependent potential pitting passivation window is the reason why the composite's rate of increase in Icorr was slower than that of the unreinforced alloy, $\Delta E = (E_{pp} - E_{corr}) \geq 100$ mV. The summary of the E_{corr} and I_{corr} values of the samples is shown in Table-3. Figure-5a, b reveals that the unreinforced sample A0 demonstrated greater resistance to corrosion than other samples, regardless of the length of time the sample was exposed to the NaCl environment. Furthermore, in contrast to samples A5, A6, and A9, sample A1, which was reinforced with 2% Al_2O_3, demonstrated superior corrosion resistance. The tiny quantity of Al_2O_3 reinforcement added to the matrix is what gives sample A1 its high corrosion resistance when compared to other reinforced samples. In comparison to samples A5 and A9, sample A6, which had 2% MoS_2 added to its matrix, demonstrated superior corrosion resistance. Nevertheless, the value obtained is significantly less than the value obtained in sample A1. One of the starting points for assaults by rusting in the NaCl environment is the existence of certain metallic oxides in the MoS_2 that is part of the matrix. Nevertheless, in the tested environment, sample A5's hybrid reinforced composites (2% Al_2O_3 and 8% MoS_2) and sample A9's (2% MoS_2 and 8% Al_2O_3) demonstrated the least amount of corrosion resistance. This suggested that 10% of the total Al matrix's hybrid reinforced substitute functioned as extremely potent pitting initiation active sites.

EIS Spectra of the Samples

Figures-6 and 7 display the Bode plots of the samples that are submerged in a 3.5% solution of NaCl for 24 and 72 hours, respectively. The samples' comparable patterns were visible in the impedance modulus against frequency Bode profile. The sample A0, which is unreinforced, possesses the greatest impedance

(Fig.-6a). At 24 hours of immersion in the corrosive environment, the strengthened composites were unable to quickly form a protective film layer like the unreinforced sample; nevertheless, the remaining samples demonstrated improved modulus of impedance after 72 hours. Figure-7a shows a constant rate of the reinforced alloy impedance modulus within the NaCl solution in relation to the values of frequency, suggesting sample without reinforcement might have demonstrated improved resistance to corrosion instead of samples that have inclusions for reinforcement.

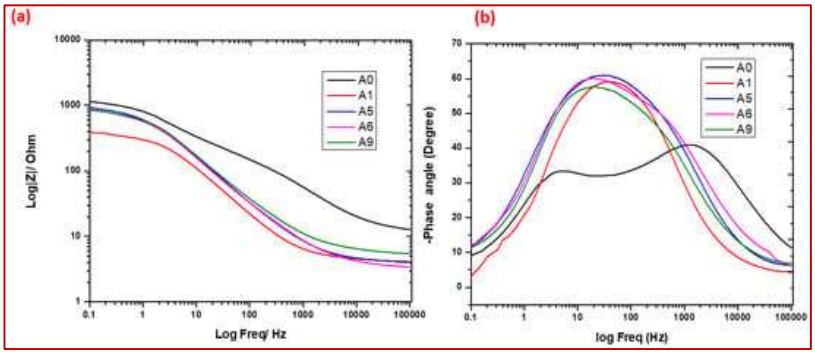

Fig.-6: (a) and (b) Samples After 24 hours in 3.5% NaCl, Bode Profiles, and Bode Phase Profiles

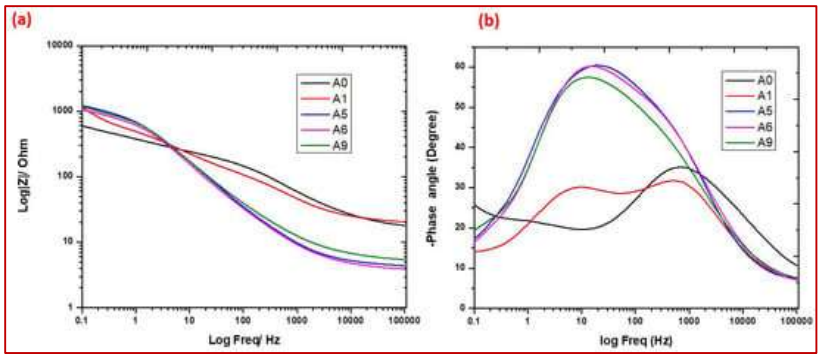

Fig.-7: (a) and (b) display the Profiles of Bode and Bode Phase of Samples in 3.5% NaCl over 72 Hours

The samples' resistance to corrosion is determined by the thin oxide layer that develops on their surfaces. This may have reduced ionic, electrical conductivity and slowed down electrochemical reactions on the sample surfaces. As can be observed for the samples dipped in the solution, samples with Greater Rct values were displayed by A1, A5, A6, and A9. from 24 to 72 hours in the 3.5% NaCl solution of immersion (Table 4). After 24 hours of immersion, the Rct values for A1, A5, A6, and A9 were 382.6, 995.3, 880.4, and 903.1 $\Omega \cdot cm^2$, respectively. After 72 hours, they increased to 979.7, 1080, 952.5, and 1040 $\Omega \cdot cm^2$. The increase in Rct values is due to two factors: the experimental setup's decreased oxygen content and the rapid development of defective corrosion results in oxide deposits on the sample surface, which may stop the solutions from having a greater effect on the samples. The prepared composite material improves the strength, wear resistance, thermal conductivity, damping capacity, a low coefficient of thermal expansion, and also reduces density, making them particularly suitable for automotive and tribological uses.

CONCLUSION

The addition of Al_2O_3 and MoS_2 improved Al 5052 alloy hardness and strength by enhancing reinforcement bonding. Corrosion in NaCl solution occurred through pitting; composites displayed similar electrochemical responses in 3.5% NaCl. Reinforcements in Al 5052 initiated rust, creating sites for corrosion. The distinct chemical properties of Al 5052's inclusions can lead to irregular oxide layer formation. This improved protection allows for composite use in less corrosion-prone areas.

ACKNOWLEDGMENTS

The authors are thankful to the principal and management of Sai Vidya Institute of Technology, Bengaluru, for their constant encouragement. Author Prutviraj R D thanks the principal and management of Rajarajeshwari College of Engineering for their valuable help.

CONFLICT OF INTERESTS

The authors declare that there is no conflict of interest.

AUTHOR CONTRIBUTIONS

The present work is related to *SDG-9: Industry, Innovation and Infrastructure.* All the authors contributed significantly to this manuscript, participated in reviewing/editing and approved the final draft for publication. The research profile of the authors can be verified from their ORCID ids, given below:

K. V. Anil Kumara https://orcid.org/0000-0003-2418-5145
R. D. Pruthviraj https://orcid.org/0000-0002-4409-4745
M. T. Swamy https://orcid.org/0000-0003-2142-3072

REFERENCES

1. I. P. Peter, M. Oki, A. A. Adeleke, B. Stojanovic, *Cogent Engineering*, **7(1),** Article: 1727167(2020), https://doi.org/10.1080/23311916.2020.1727167
2. A. A. Adeleke, I. P. Peter, K. O. Jamiu, B. B. Olujimi, A. J. Okolie, *Materials Today: Proceedings*, **46(12),** 5909(2021), https://doi.org/10.1016/j.matpr.2021.03.537
3. P. Omoniyi, O. Abolusoro, O. Olorunpomi, T. Ajiboye, O. Adewuyi, O. Aransiola, E. Akinlabi, *Journal of Composites Science,* **6(7),** 189(2022), https://doi.org/10.3390/jcs6070189
4. I.P. Peter, M. Oki, A. A. Adeleke, O. O. Agboola, *Scientific African*, **12,** e00839(2021), https://doi.org/10.1016/j.sciaf.2021.e00839
5. S. Nanjan, J. G. Murali, *Materials Research,* **23(2),** 1(2020), https://doi.org/10.1590/1980-5373-MR-2019-0681
6. I. P. Peter, M. Oki, A. A. Adeleke, P. O. Omoniyi, *Scientific Reports,* **11,** Article number: 14845(2021), https://doi.org/10.1038/s41598-021-94420-0
7. M. Imran, A. R. A. Khan, *Journal of Materials Research and Technology*, **8(3),** 3347(2019), https://doi.org/10.1016/j.jmrt.2017.10.012
8. G. Singh, N. Sharma, *Composites Part C: Open Access*, **4,** 100106(2021), https://doi.org/10.1016/j.jcomc.2021.100106
9. P. Omoniyi, A. Adekunle, S. Ibitoye, O. Olorunpomi, O. Abolusoro, *Journal of King Saud University - Engineering Sciences,* **34(6)**, 445(2022), https://doi.org/10.1016/j.jksues.2021.01.006
10. I. P. Peter, M. Oki, A. A. Adeleke, P. Omoniyi, E. Ajisegiri, E. Akinlabi, *Acta Metallurgica Slovaca,* **28(1),** 25(2022), https://doi.org/10.36547/ams.28.1.1340
11. N. H. Ononiwu, C. G. Ozoegwu, N. Madushele, O. J. Akinribide, E. T. Akinlabi, *Biointerface Research in Applied Chemistry*, **12(4),** 4900(2022), https://doi.org/10.33263/BRIAC124.49004919
12. P. Omoniyi, O. Abolusoro, O. Olorunpomi, T. Ajiboye, O. Adewuyi, O. Aransiola, E. Akinlabi, *Journal of Composites Science*, **6(7),** 189(2022), https://doi.org/10.3390/jcs6070189
13. K. C. Satish, V. Kumar, S. Prasad, P. S. Kiran, O. S. A. Rahman, P. Singh, S. Indupuri, R. Shrivastava, S. M. Pandey, A. K. Keshri. *Materials Today Communications*, **36**, 106640(2023), https://doi.org/10.1016/j.mtcomm.2023.106640
14. M. A. Nahr, S. E. Mirsalehi, A. Papi, *Journal of Materials Research and Technology*, **36,** 8609(2025), https://doi.org/10.1016/j.jmrt.2025.05.124
15. G. Perumal, N. Senthilkumar, N. Naik, B. Deepanraj, *Discover Applied Sciences,***7**, Article number 237(2025). https://doi.org/10.1007/s42452-025-06687-x

[RJC-9327/2025]